Proceedings of the 2003 IEEE International Frequency Control Symposium and PDA Exhibition
Jointly with the 17th European Frequency and Time Forum

IEN-CsF1 ACCURACY EVALUATION AND TWO WAY FREQUENCY COMPARISON

F. Levi, L. Lorini, D. Calonico, E.K. Bertacco and A. Godone
Istituto Elettrotecnico Nazionale "G. Ferraris", Torino Italy

*Abstrac*t – **In this paper we report the accuracy evaluation of the Italian primary frequency standard IEN-CsF1. We discuss the frequency shifts our frequency standard is corrected for and the procedure used for accuracy evaluation. In the last section we report a frequency comparison against two remote laboratory, the National Institute of Standard and Technology and the Physikalisch-Technische Bundesanstalt using the two way comparison technique.**
Keywords **- Primary frequency standard, Atomic Fountain, TWSTFT**

I. INTRODUCTION

Laser cooling techniques [1] had a great impact on the development of high accuracy atomic frequency standards. The old concept of atomic fountain, firstly attempted by Zacharias, could be eventually developed with great success. Several fountains and laser cooled devices were developed some used as primary frequency standards [2,3,4,5], some for the realization of gravitometers or gyroscopes [6], and finally fountains were used also for precise measurement of fine constant time variation ($\dot{\alpha}/\alpha$) [7] or to investigate collision theory [8] .
IEN has developed a Cesium fountain to be used as a primary frequency standard [9]. The accuracy level achieved by Cesium fountain frequency standards is the highest among any other measurement currently available and reach a relative uncertainty level of 10^{-15}.
The principle the atomic fountain rely on to achieve a high accuracy is to enlarge the measurement time of the clock transition (increasing the atomic quality factor), and to reduce the absolute value of many shifts, by the use of nearly mono-kinetic ultra-cold atoms.
IEN- CsF1 is not operated as a clock but as a frequency standard, thus it possible to compare our fountain to another one by simultaneous measurement of the same reference clock. We have done a remote comparison with NIST-F1 of National Institute for Standard and Technology (USA), and with CSF1 of Physikalisch-Technische Bundesanstalt (PTB) Germany, by means of the two way satellite time and frequency transfer (TWSTFT) technique, measuring the same Hydrogen maser (IEN HM1), that was also used as local oscillator for our fountain.

II. SYSTEM DESCRIPTION

IEN-CsF1 is composed of four main parts, the optical bench, the fountain structure, the control electronics and the synthesis chain.
The fountain structure: the fountain structure (figure 1) is composed of three parts, a trapping, a detection and an interaction region.
The trapping region is simply a multiport vacuum cross where the various laser beams intersect in the middle; the cesium vapor is created by a small oven with a big and short nozzle (2 x 2 mm diameter and length). The detection region is above the trapping one and is composed of two identical interaction zones where differential optical detection of the population in each F ground state level can be accomplished.
A second detection zone below the trapping region (shown in fig 1) is not used in this work.

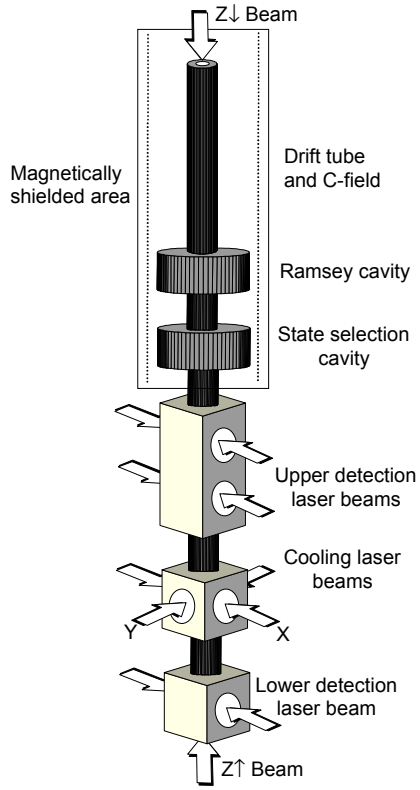

Figure 1- Fountain set up

Between the trapping and the detection regions a graphite bottleneck avoids cesium vapor flowing in the upper part of the fountain, maintaining then the required differential vacuum level.
The collection efficiency of the fluorescence emitted by the atoms crossing the laser beam in their flight is ≈17%.
The interaction region is the most complex part of the physical apparatus, it is composed of two microwave cavities and a drift tube, realized in OFHC copper, the cavities and the tube are also part of the vacuum structure.
The two cavities are vertically aligned and spaced by 10 cm, the first one is used in the state selection procedure, while the second one is the Ramsey cavity used for the clock interaction.

The cavities [10] are cylindrical and resonant on the TE_{011} mode with a squeezed geometry on the vertical axes ($h = 2.5$ cm, $\phi = 6$ cm). The atoms can pass through the cavity by means of a below cut off cylindrical waveguide. The drift tube is a one meter long region where the atoms travel during the ballistic flight. Outside the interaction region there is the heater, the C-field map coils, the C-field solenoid and four coaxial layers of magnetic shields. At the top end of the drift tube is placed a below cut-off waveguide to avoid microwave leakage in the vacuum system.

The optical system (figure 2) is composed of four laser diodes: a master, a repumper and two slaves. The master laser is offset-frequency locked (with Pound Drever technique) on the $6S_{1/2}$, F=4, $6P_{3/2}$ F=5 cycling transition of ^{133}Cs. The laser beam is then amplified by means of two slave lasers capable of 150 mW each, while the residual light of the master laser is used in the detection system The slave lasers produce the X-Y and the Z↓ Z↑ beams respectively. The cooling beam are expanded and they are spatially filtered by pin-holes or optical fibers; the average light power density is of few mW/cm^2.

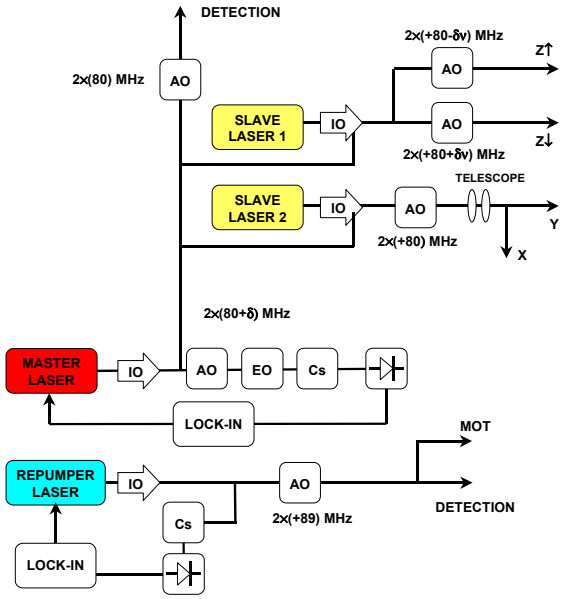

Figure 2 – Optical bench scheme. AO Acousto-Optic Modulator, EO ElectroOptic modulator, Cs Cesium cell, IO Optical Isolator

The cycling transition is not completely closed because of nearby levels, therefore a repumper beam is required in the trapping region to maintain the atoms coupled to the laser cooling cycle. The repumper beam is frequency locked on the $6S_{1/2}$, F=3, $6P_{3/2}$ F=4 pumping transition. Part of the repumper light is used in the detection region as well.

All the laser beams are double passed inside Acusto-Optic modulators (AO) to fine tune the laser frequencies, to allow frequency sweeps and power control, as required in the subd-Doppler cooling cycle.

Electronic Control: the electronic has two main tasks, 1) timing of the fountain operation sequence and 2) signal elaboration and digital servo control system. Three boards inside a PC (pattern generator, AD/DA converter and GPIB) are in charge of the various control functions.

The pattern generator drives the sequence used for the fountain operation, as will be described in the following paragraph. The frequency servo system uses the atomic signal to measure the transition probability and change the central frequency of a DDS in accordance with the experimental data.

Synthesis chain

We use a direct frequency multiplication chain driven at 5 MHz by a BVA quartz oscillator, phase-locked to an H-maser; its output at 9.2 GHz is mixed with the output of a DDS at ~12 MHz, to reach the Cs hyperfine frequency. The frequency accuracy of the DDS is 2×10^{-13} giving an accuracy of the synthesis chain better than 2×10^{-16}.

The phase noise of the synthesized frequency set an upper limit to the frequency stability at about $1.5\times10^{-13}\,\tau^{-1/2}$

III. Operation Cycle

The operation cycle of the fountain is performed in several steps: atom loading, density lowering, launching, sub-Doppler cooling, state selection, Ramsey interaction and detection.

The loading step in our fountain is done with a MOT followed by a free expansion-recapture sequence [11], where the initial cloud density is lowered. During this stage, the MOT magnetic field is switched off and the laser beams are alternatively switched on and off, taking advantage for the cloud expansion of the relatively high temperature of the atoms before the post cooling. After the expansion the atomic cloud is a sphere of 1cm diameter (limited mainly by the vertical beam dimensions, defined by the microwave cavity holes).

The launch and post-cooling stages happen together, first the Z laser beam frequencies are switched to the launch configuration (blue detuning of the lower beam and red detuning of the upper), and after 1 ms all the laser frequencies are swept out of resonance and the amplitudes are ramped down cooling the atoms close to 1 μK.

The lasers are then switched off by means of AOs (fast switching) and mechanical shutters. The atoms enter the state selection cavity where a microwave pulse transfers the atoms in $6S_{1/2}$ F=4, m_F=0, into $6S_{1/2}$ F=3, m_F=0; a strong laser pulse resonant with the $6S_{1/2}$ F=4 state removes then all the remaining atoms and destroy the coherence created by the first microwave pulse. The atoms enter the Ramsey cavity, reach their apogee and fall down upon gravity undergoing the second microwave interaction on their way down.

The atomic sample is then interrogated in the detection region by means of a differential detection scheme. This scheme is very powerful since gives directly the transition probability, and therefore rejects the noise due to the fluctuations of the loaded atom number. First a standing

wave laser beam tuned on the cycling transition detects the atoms in F=4 state, a progressive wave sweeps off the detected atoms, a repumper beam pumps the atoms in F=3 into F=4 and finally a second standing wave laser beam on the cycling transition, with the same detection efficiency of the first one, detects the atoms that were in F=3. Indicating with S_i the signal obtained by atoms in the i state, the transition probability is given by: $P= S_4/(S_3+S_4)$.
The servo system uses square wave frequency modulation, a first measurement cycle is done *e.g.* on the left side of the central Ramsey fringe (P_L) and a second on the right one, (P_R) the two transition probabilities are then compared and the central frequency of the synthesizer is corrected according to the formula

$$\delta\nu = (P_R - P_L)\ \Delta\nu_A\ G \qquad (1)$$

where $\Delta\nu_A$ is the clock transition linewidth and G is the gain of the digital loop.
The sequence of frequency values of the DDS gives the frequency difference between the fountain and the local oscillator.

IV. Main Biases

IEN-CsF1 frequency is corrected for four physical effects: 2nd order Zeeman, blackbody radiation, gravitational red shift and atomic density. Other effects deriving from null shift experiments such as microwave leakage, microwave power and spectrum, light shift, neighboring lines pulling are not corrected for. Finally effects whose calculated shift is well below 10^{-15} are not corrected for as well, this is the case of cavity pulling, Doppler effect (classic and relativistic), cavity distributed phase shift, Majorana transitions, background gas.

A. Magnetic Field second order Zeeman.

We use two different methods to evaluate the Zeeman effect in our fountain. First, we excite low frequency transitions (ΔF=0, Δm_F=1) when the atoms are at apogee, switching on for 100 ms a couple of long rectangular coils placed along the drift tube. The frequency of the transition is proportional to the local value of the field B according to the relation $\nu = k_Z B$, with k_Z=350.98x10^7 Hz/T.
This method gives a measurement of the value of the field at a given point. Launching atoms at various height provide a complete information of the field map.
Second, we detect the Ramsey central fringe position on the magnetic sensitive F=3, m_F=1 to F=4, m_F=1 transition (denoted as 1-1) at increasing launching height.
The two methods differ qualitatively since the first measures the magnetic field value locally, while the second gives the information on the (temporal) average value of the field as seen by the atoms along different trajectories. The first method is particularly suited to the fountain where apogee of the trajectory can be fixed very precisely by adjusting the launching parameters. The resulting precise map of the local magnetic field gives better results in the evaluation of the quadratic Zeeman shift of the clock transition by avoiding the uncertainty between $\langle B^2 \rangle$ and $\langle B \rangle^2$.
In figure 3 a C field map is reported with a nominal applied field of 98 nT.

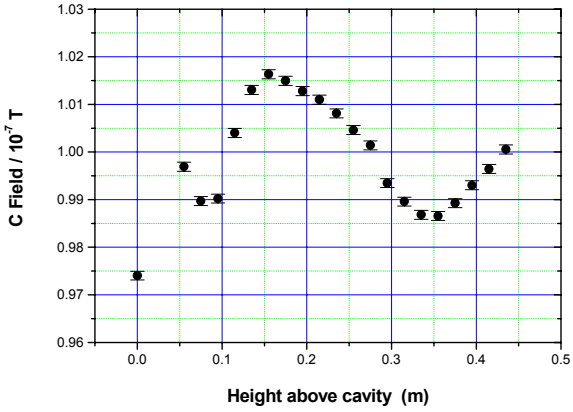

Figure 3 – C-field map

We can use the map shown in figure 3 to predict the location of the 1-1 fringe by integrating the magnetic field with respect to time. The resulting prediction is compared to experimental data in figure 4. The disagreement is less than 3×10^{-4}, relative to the linear Zeeman frequency shift, and decreases significantly when atoms are launched more than 30 cm above the cavity, where the maximum of inhomogeneities are located validating thus the technique.

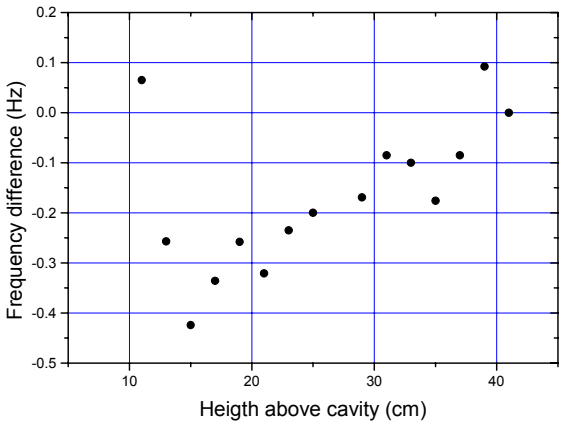

Figure 4 – Difference between measured and calculated frequency of the central fringe of the magnetic sensitive (1-1) transition

The relative stability of the magnetic field has been measured locking the fountain onto the 1-1 line, is less than 2x10^{-5} for integration periods varying from 100 s to 10^5 s.
The field variation, due to the temperature control of the room, gives a periodic peak to peak relative fluctuation of 7×10^{-5} that can be conservatively assumed as the uncertainty

of the field knowledge. In usual operating conditions the Zeeman shift correction is therefore $(-4.251\pm0.003)\times 10^{-14}$.

B. Atomic Density

As described in[11], in IEN-CsF1 atoms are launched after a free expansion phase and then state selected (the atoms begin the Ramsey interaction in F=3, m_F=0).

The free expansion loading technique results in a larger amount of atoms collected than in a full molasses approach. In spite of this increase in atoms number, the atomic density is rather like in a molasses, much smaller than in the full MOT approach. Moreover, we get a high spherical symmetry for the atomic sample that allows simple modeling of the cloud flight across the drift tube.

Other significant advantages of this implementation are the possibility to decrease the dead time in the fountain duty cycle by faster trapping and the possibility to improve differential measurements: in fact, higher is the density variation, more accurate and simpler is the evaluation of the zero density extrapolation.

We assume a linear dependence between the detected signal and the atomic density and we use a two point differential method: a frequency measurement at high density (HD) is alternated with a low density one (LD) with typical density ratio of $n_H/n_L=S_H/S_L=3$. Here n_H (n_L) and S_H (S_L) are respectively the density and the signal detected in the high (low) density case. The measurement is performed running the fountain *e.g.* one hour in the LD configuration and one hour in the HD state, and measuring the fountain frequency against the local oscillator in the LD (ν_L) and in the HD state (ν_H). During this integration time, the drift of our Hydrogen Maser IEN-HM1 doesn't affect the differential measurement at the 10^{-16} level.

The low density collisional bias $\Delta\nu_C$ is evaluated by the simple relation

$$\Delta\nu_C = S_L(\langle\nu_H - \nu_L\rangle)/(S_H - S_L) \qquad (2)$$

where $\langle\nu_H - \nu_L\rangle$ is the average of the difference $\nu_H - \nu_L$ over the whole integration time.

The amplitude stability of the detected signal is better than 10% over 10 days of measurement and approaches 2% over 1 day. The uncertainty of the differential frequency measurement is less than 50%. The atomic density shift turns out to be $(3\pm1.5)\times10^{-15}$ for typical operating conditions.

C. Blackbody

Three thermocouple sensors are placed along the interaction region: one on the cavity body, one where the atoms reach their apogee, and one at the top of the drift tube. The temperature of our cavity is 69.5° C, for tuning purposes. The maximum temperature offset seen by the atoms during the ballistic flight is 0.5K. The temperature of the cavity is electronically controlled and its stability is better then 20 mK.

This results in a blackbody radiation shift of $(-26.7\pm0.3)\times10^{-15}$ [12].

D. Gravitational Potential

The elevation of the IEN-CSF1 interaction region respect to the geoid is 292.01 m as reported by a measurement done by the "Stazione Astronomica" of Cagliari [13]. Hence the Gravitational red shift correction we apply to the fountain frequency is $(29.3\pm0.1)\times10^{-15}$.

However it is worth remind that gravitational red shift is not a relevant frequency shift for proper time (and therefore strictly speaking does not affect the accuracy of a primary frequency standard), but it becomes important for coordinate time and remote comparison with standards situated at different gravitational potentials.

E. Null Shift Experiments

In the fountain operation there are several phenomena, typically due to imperfections in the excitation or in the system realization, that can produce unwanted shifts; the absence of this shifts must be carefully verified with "null shift experiments". With null shift experiment we indicate a differential measurement where we compare the frequency difference between the usual configuration and a second configuration where a given phenomenon is strongly enhanced. This measurement allows to give an upper value to the examined shift.

During a fountain evaluation we perform the following "null shift experiments":

1) Microwave leakage/spectrum; this is the classical experiment where a measurement with $\pi/2$ pulse is alternated with a *e.g.* $5\pi/2$ pulse.
2) Presence of neighboring lines; the fountain is locked *e.g.* on the 5th fringe right and on the 5th fringe left
3) Residual light shift; the shutter on the injection beam of the slaves is removed, the light is therefore much closer to optical resonance and the light shift is expected to be higher.
4) Unwanted synchronous effect; we change the duty cycle and the launching height.
5) Residual microwave in the state selection cavity; we change the state selection frequency half linewidth higher or lower.

None of these experiments allowed to observe significant shift at the 10^{-15} level.

F. Other effects

The following effects give a calculated shift not significant at the 10^{-16} level and the fountain is not corrected for:

1) Cavity pulling: The cavities are tuned with temperature closer than 100 kHz to the atomic resonance, a conservative estimation of the cavity pulling effect (considering the worst possible experimental conditions) gives the negligible value of 10^{-16}.
2) Doppler effect (classical and relativistic): the maximum speed of the atoms during the interaction is less than 3 m/s (and the average velocity is much less) the resulting Doppler shift is $1.6\text{x}10^{-18}$. The first order Doppler is an effect due to the residual travelling wave in the cavity,

the amount of this effect has been estimated to be $<1\text{x}10^{-17}$.

3) Majorana transitions: IEN CsF1 is state selected inside the magnetically shielded region and the maximum relative magnetic field variation seen by the atoms is of $3\text{x}10^{-2}$. Assuming an atomic velocity of 3 m/s over the whole trajectory of about 0.4 m, we obtain that the adiabatic condition [14] is satisfied by a factor 2000 thus resulting in a potential frequency shift of $1\text{x}10^{-16}$ [15].
3) Background Gas: the background pressure of the vacuum system is estimated from the Ion pump current and is below 10^{-9} Torr. The shift effect of soft collisions with background gas is in the 10^{-16} range as well.
4) Phase shift: the geometry of our Ramsey cavity gives a maximum phase variation across the hole off 0.5 µrad [10]. Thus the maximum shift in the unlikely situation where all the atoms experiment the maximum phase variation between way up and way down is $3\text{x}10^{-17}$.

TABLE I
ACCURACY BUDGET OF IEN-CSF1

Effect	Bias ($\text{x}10^{-15}$)	Uncertainty ($\text{x}10^{-15}$)
2nd Zeeman Shift	-42.51	0.03
Blackbody Radiation	26.7	0.3
Atomic Density	3	1.5
Gravitational Potential	-25.8	0.1
Others Effects	-	< 1
Total	-4.1	1.8

V FREQUENCY STABILITY

The stability of a primary frequency standard is important to the extent that allows to perform high resolution measurements in a reasonable time.

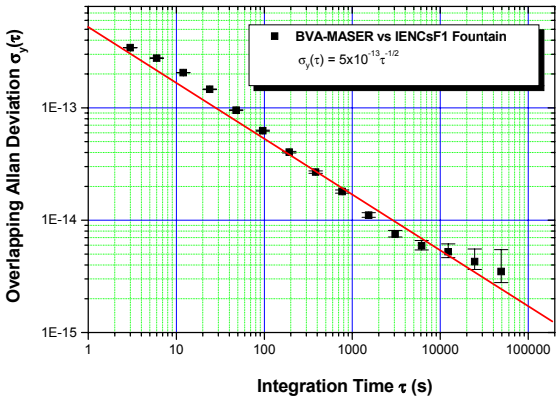

Figure 5 - Frequency stability of IEN-CsF1

In our case the stability is limited by the noise of the local oscillator; therefore we can operate the fountain with a relatively low atomic density without compromising the short term stability.

The stability we obtain extrapolating at 1 s the white noise level of the frequency standard is $\sigma_y(\tau) = 5\times10^{-13}\tau^{-1/2}$

In figure 5 is reported the stability of our fountain: the long term behavior is due to the Maser frequency drift. Its relatively high value is due to the fact that our maser is new and its drift is still very high ($\approx 4\times10^{-15}$/day)

VI REMOTE FREQUENCY COMPARISON

The TWSTFT has demonstrated to be a powerful technique for long distance frequency transfer [16]. Moreover its performance on medium term stability (1 day to 1 week integration time) is notably higher than the GPS common view technique and is particularly suited for remote fountain comparison.

IEN routinely operates the TWSTFT measurements following the BIPM schedule (3 days per week) and the measurement are currently used to link IEN clocks to TAI via UTC(IEN).

The TWSTFT system at IEN is composed by a Ku-band transceiver, a MITREX modem and a high resolution time interval counter; all the measurement procedures are automated via computer. To run the primary frequency comparison experiment the modem was fed by the IEN-HM1 frequency. With this setup no internal measurements are required to relate the fountain and the TWSTFT measurements; however the TAI link is kept using the internal measurement between UTC(IEN) and the H maser.

At NIST the TWSTFT equipment is driven by UTC(NIST), which is actually a steered H maser; in this case internal measurements are used to relate the UTC(NIST) to the maser connected with the fountain.

At PTB the TWSTFT system is driven by an H-maser and referred to UTC(PTB) with internal measurements, the H-maser is also connected to the fountain with frequency comparison.

The IEN maser drift is evaluated with a quadratic fit as $4\cdot10^{-15}$/day and the fit residuals are shown in fig. 6.

A quantitative analysis of the stability of the TWSTFT link is difficult at the moment, because only a short data period is available (60-days).

However a preliminary analysis is possible, particularly for short integration periods. The Allan standard deviation has been calculated for τ = 2, 7 days using a non-overlapping algorithm for τ = 2 days (data are non equally spaced) and an overlapping algorithm for τ = 7 days.

The value obtained are:

$$\sigma_y(2d) = 3\cdot10^{-15},$$
$$\sigma_y(7d) = 4\cdot10^{-15}.$$

The 2 day value agrees with the value reported in [16] and is probably representative of the actual link noise; on the contrary the 7 days value is limited by the oscillators noise.

The primary frequency comparison uses a 14-days long period during which the IEN fountain operation approached the 98% of the available time. In parallel we used 8 TWSTFT measurements from the BIPM schedule together

with some extra schedule measurements on Tuesdays and Thursdays (only with NIST). For 1 day interval TWSTFT measurement a $6 \cdot 10^{-15}$ uncertainty is assumed (Figure 7).

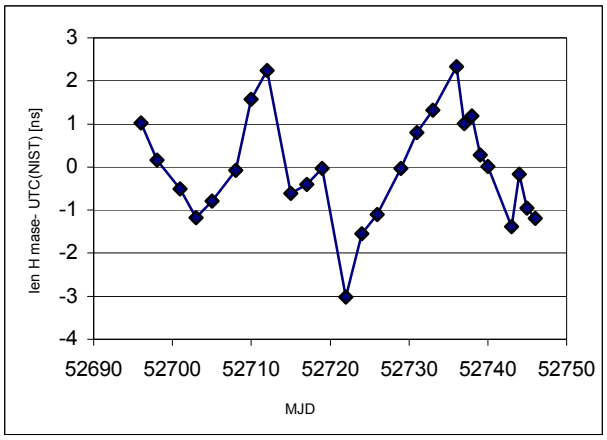

Figure 6 – Time differences between IEN H maser and UTC(NIST). Drift removed

Taking into account the average frequency on the whole period the result is:

$$\langle y(\text{NIST F1})\rangle - \langle y(\text{IEN CsF1})\rangle = (-4 \pm 4)\cdot 10^{-15}$$

$$\langle y(\text{PTB CSF1})\rangle - \langle y(\text{IEN CsF1})\rangle = (2.6 \pm 4)\cdot 10^{-15}$$

The uncertainty is comprehensive of all the various contributions, that are: fountains uncertainty, link uncertainty, propagation uncertainty.
In fact in the case of NIST, the frequency of the time scale used in the comparison is extrapolated out of the last NIST-F1 calibration by means of the NIST maser ensemble.

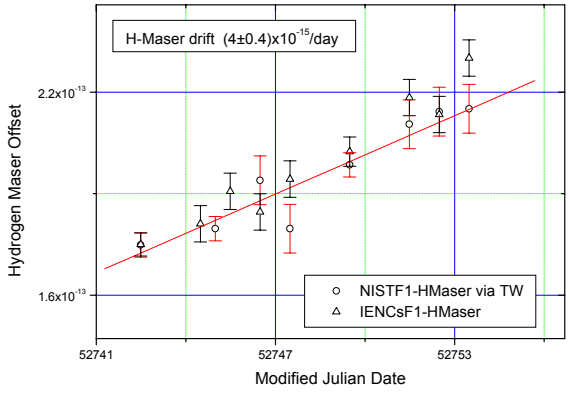

Figure 7 - IEN H maser frequency measurements versus IEN CsF1 and NIST F1 (via TWSTFT)

VII Conclusions

We have realized a Cesium fountain primary frequency standard and we have evaluated its accuracy to be 1.8×10^{-15}, limited mainly by the spin exchange collision shift.

With the aid of the TWTFT, that allow to perform a remote measurement of the average frequency of our H-maser on a given time period, we have done a frequency comparison between our primary frequency standard ant those of NIST and PTB, showing a good agreement well inside the error bars of the comparisons.

Acknowledgments

We are grateful to Valerio Pettiti and Franco Cordara for their help in the TW comparisons. We thank Steve Jefferts for his contribution to the realization of the fountain Thomas Parker for the calculations made for the remote comparison with NIST-F1 and Stefan Weyers for the comparison with PTB-CsF1.

References

[1] AA. VV. laser cooling and trapping of atoms, Josa B 6 11 1989
[2] A.Clairon, S. Ghezali, G. Santarelli, P. Laurent, S. Lea, M. Bahoura, E. Simon, S. Weyers, K. Szymaniec, "Preliminary accuracy avaluation of a cesium fountain frequency standard", *Proc. of 5th Symp. on Freq. Stand. and Metr.*, Woods Hole, MA, 1997.
[3] S. Jefferts, *et al*. accuracy evaluation of NIST- F1, *Metrologia*, **39**, 321-336, 2002.
[4] S. Weyers, U. Huebner, R. Schroeder, C. Tamm and A Bauch, "Uncertainty evaluation of the atomic caesium fountain CSF1 of the PTB" *Metrologia*, vol. 38, pp. 343-352, 2001
[5] K. Gibble and S. Chu, Laser-cooled Cs frequency standard and a measurement of the frequency shift due to ultracold collisions, *Phys Rev. Lett.* ,70, 1771-1774, 1993.
[6] A. Peters, K Y. Chung, and S. Chu, "High precision gravity measurements using atom interferometry" *Metrologia*, vol. 38, pp 25-61, 2001.
[7] H. Marion *et al*. Search for Variations of Fundamental Constants using Atomic Fountain Clocks, *Phys. Rev. Lett*. 90, 150801 2003
[8] Y. Sortais, S. Bize, C. Nicolas, G. Santarelli and A. Clairon, "87Rb versus 133Cs in cold atom fountains: a comparison", *IEEE Trans on UFFC* vol. 47, n. 5, pp. 1003-1007, Sept. 2000.
[9]F. Levi *et al.* Preliminary accuracy evaluation of the IEN CS fountain, proceedingso fo the 2001 EFTF, p 104, Neuchatel 2001
[10] S. R. Jefferts, R. E. Drullinger, A. De Marchi, "NIST cesium fountain microwave cavities" *Proc. of IEEE Freq. Contr. Symp.* 1998, pp. 6-8
[11] F. Levi, L. Lorini, D. Calonico, A. Godone, Systematic shift uncertainty evaluation of IEN CSF1 primary frequency standard, *IEEE Trans. on Instr. and Meas*. **52** 2 2003
[12] A. Bauch and R. Schroeder, "Experimental verification of the cesium hyperfine transition frequency due to blackbody radiation" *Phys. Rev. Lett.*, vol. 78, n. 4 , pp. 622-625, 1997.
[13] A. Banni, L. Mureddu, "Collegamento in rete geodetica tra i principali laboratori italiani di tempo e frequenza", *Cagliari Astronomic Station,* Internal Report, 1999
[14] J. Vanier, C. Audoin, *The Quantum Physics of Atomic Frequency Standards,* Bristol/Philadelphia, Adam Hilger, 1989.
[15] A. Bauch , R. Schroder, *Ann. Physik,* **2**, 421-449, 1993.
[16] T. Parker, P. Hetzel, S. Jefferts, S. Weyers, L. Nelson, A. Bauch, J. Levine, "First comparison of remote cesium fountains" *Proc. of 15th EFTF*, Neuchatel 2001, pp 57-71